

## 1. Introduction

The number of diamondiferous kimberlites in North America has increased dramatically over the last ten years. We estimate the population of kimberlites in Canada and US to be more than 850, where about 455 kimberlites are considered diamondiferous – contain at least microdiamonds (Faure, 2006). This large number of new discoveries now makes it possible to apply empirical mineral mapping techniques to diamond exploration. We present a continental-scale mineral potential model for diamondiferous kimberlites in North America based on an artificial neural network, which uses regional geophysics as inputs and the location of known diamondiferous kimberlites as data to be modeled.

## 2. Mineral potential mapping technique

We have used a data-driven technique to model diamondiferous kimberlites favorability. This technique directly uses the input data to deduce the rules that govern the location of known mineral deposits based on a set of input layers. In data-driven techniques such as artificial neural networks, expert knowledge is required to determine which input layers are likely to be important to the model, even if the exact way in which each layer should contribute to the potential mapping is not known.

## 3. Artificial neural networks

Artificial neural networks are a powerful data-driven technique that is loosely based on the structure and interactions of biological neurons. Each artificial (or biological) neuron is a simple entity that performs a very basic processing. It is the connection of these basic components in large networks that provide powerful data processing capabilities to the networks. Just like their biological counterparts, artificial neural networks can "learn" from examples is provided to them and apply this learning to new cases for which the result is not known. In a mineral potential mapping project, a neural network can "learn" to recognize the combination and characteristics of a given set of input geoscientific layers that best explain the location of known deposits vs. "barren" areas and evaluate the mineral potential of all cells based on the learning process. Examples of applications of neural networks in mineral potential mapping can be found in several studies (Pan and Harris, 2000; Singer and Kouda, 1996; Brown et al., 2000; Bougrain et al., 2003).

## 4. Study area

The mineral potential model covers most of Canada and the U.S. (Fig. 1). The model is restricted to emerged areas and to adjacent marine continental platforms. The model is also restricted by the availability of some of the input layers.

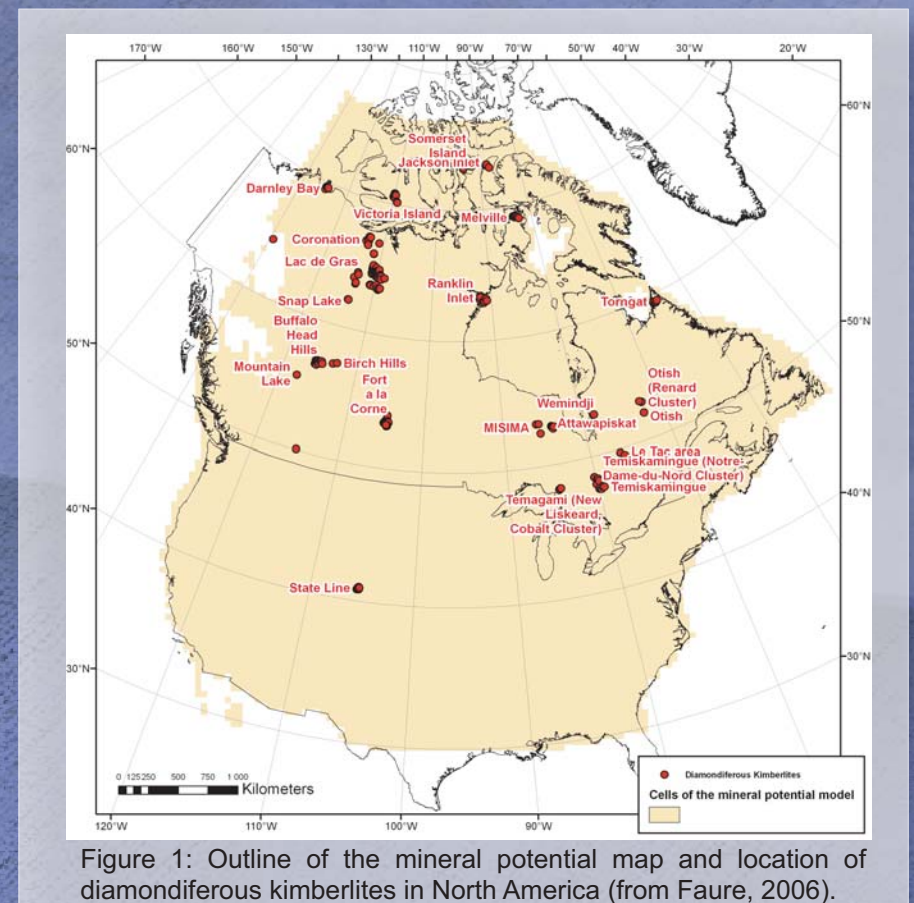


Figure 1: Outline of the mineral potential map and location of diamondiferous kimberlites in North America (from Faure, 2006).

## 5. Location of diamondiferous kimberlites in North America (target layer)

The location of 419 diamondiferous kimberlites in North America has been used as the target layer for the mineral potential model (Fig. 1).

## 6. Raw and derived input layers 3D mantle tomography

Seismic tomography gives a 3D snap shot of the actual relative variation in composition and temperature of the mantle (Fig. 2). High velocity anomalies characterize relatively low temperatures and highly depleted mantle of cratonic root, whereas low velocities is the signature of younger metasomatized or tectonically active regions. The shear wave velocity model of Godsey et al. (2003) for the uppermost mantle beneath the North America has been used for this study. The three dimensional velocity structures are imaged down to 250 km. Relative high velocities (+6%) characterize Archean sub-cratonic lithosphere and persist down to 230 km beneath Lac de Gras. Low velocities (-7%) characterize the tectonically active western Cordillera. Slices at 10km depths intervals between 30km and 250km were used as inputs to the mineral potential model (Fig. 3). Horizontal velocity gradients maps at each depth have also been calculated and used in the model (Fig. 4).

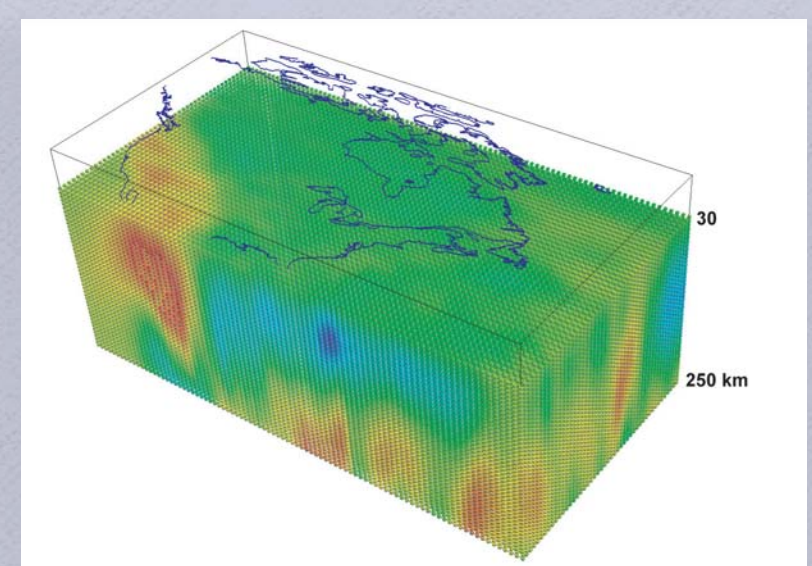


Figure 2: 3D block model of Raleigh wave phase velocity perturbations for North America.

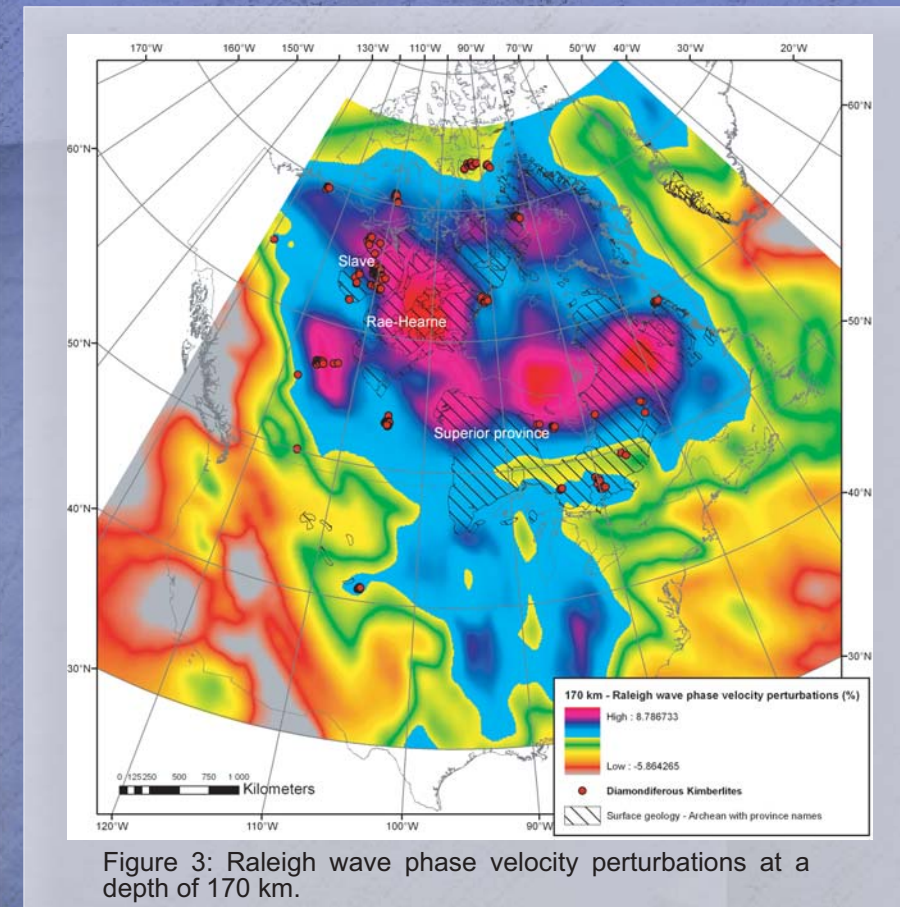


Figure 3: Raleigh wave phase velocity perturbations at a depth of 170 km.

## Bouguer Gravity anomalies

Bouguer gravity anomalies are induced by variations in crustal and mantle density and thickness. On the continental domain, lowest gravity anomalies reflect tectonically active region such as the Cordillera and the Basin and Range (Fig. 5). Globally, Archean cratons show lower gravity anomalies than surrounding younger terranes.

## Moho depth

The Moho topography preserve features reflecting the tectonic processes of the lithosphere (Fig. 6). The seismic Moho's depth is 27 km beneath the most recently accreted crust, thickens beneath the plutonic suture zone from 30 to 36 km depth, and then remains almost entirely within the depth range of 33-36 for the stable part of the continent (Clowes et al., 2005). Significant changes in Moho depth occur at tectonic subduction zones and rifted margins (active and preserved). Data source comes from model Crust 5.1 of Mooney et al. 1998.

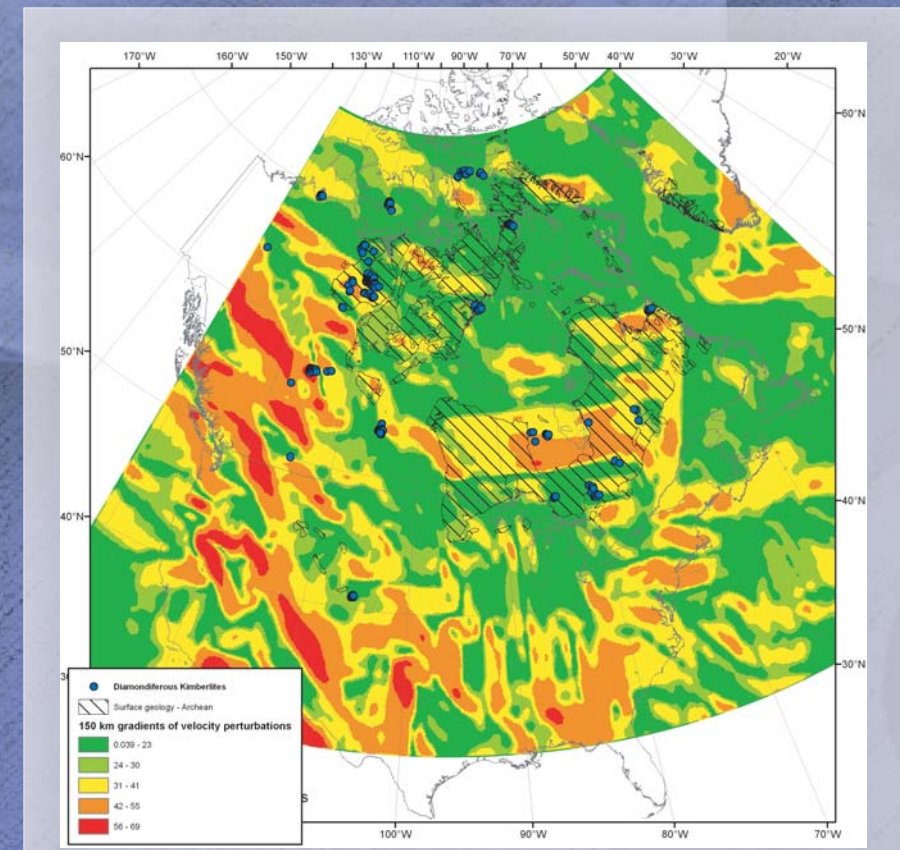


Figure 4: Horizontal gradients of Raleigh wave phase velocity perturbations at a depth of 150 km.

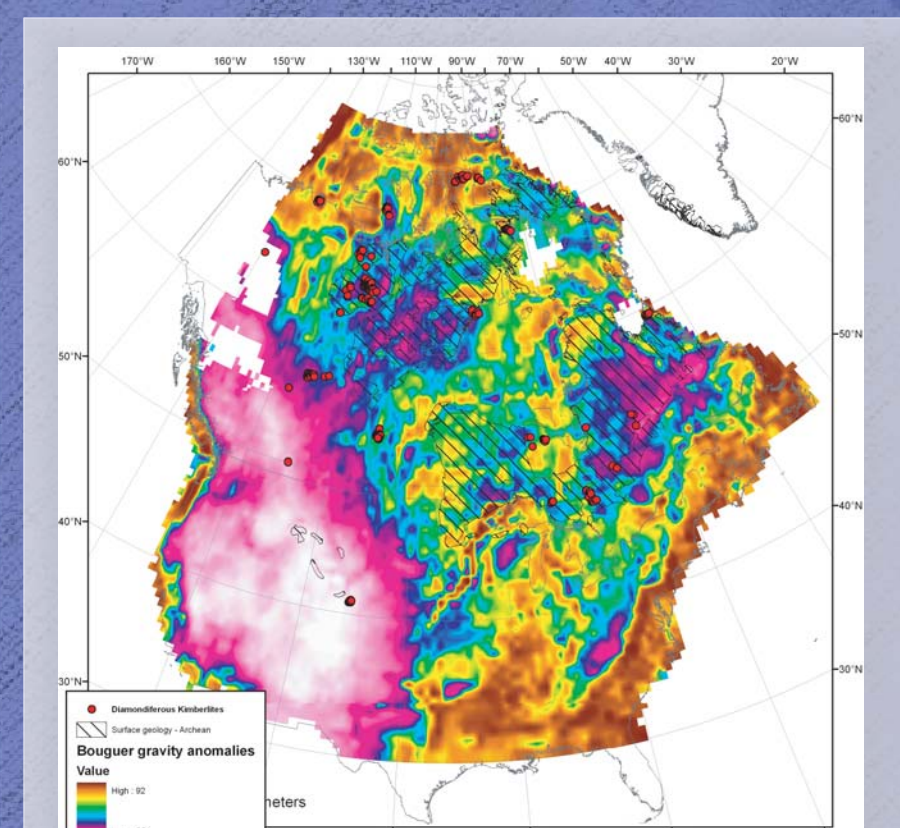


Figure 5: Bouguer gravity anomalies. (source: DNAG, 1989).

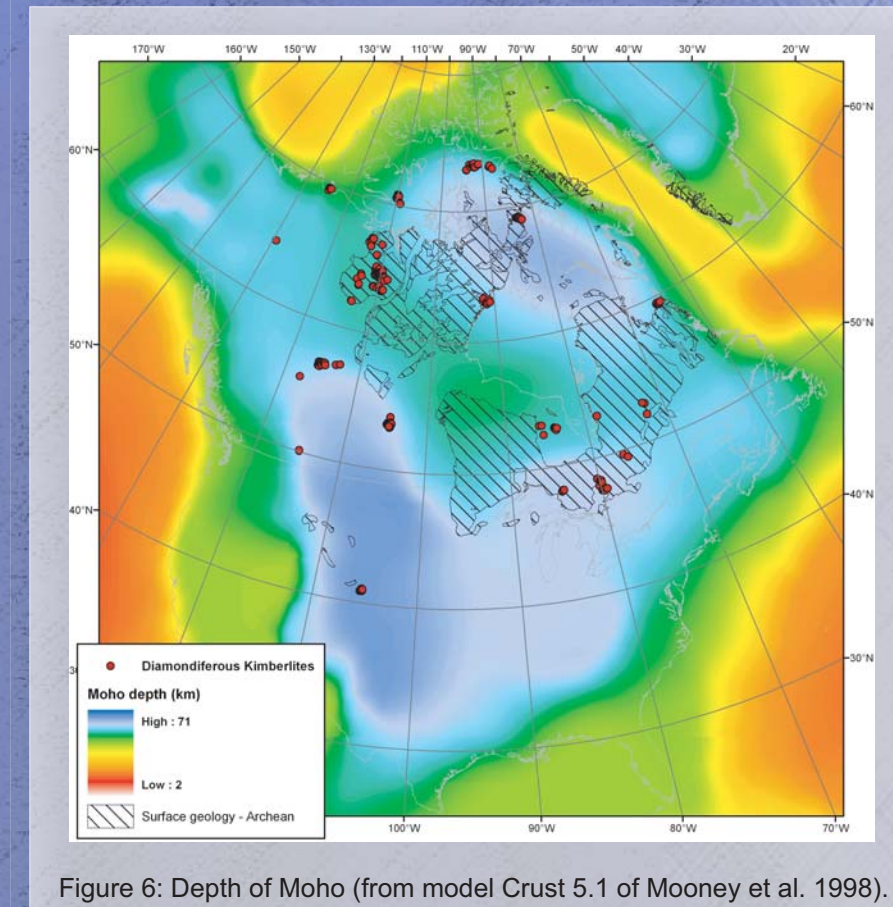


Figure 6: Depth of Moho (from model Crust 5.1 of Mooney et al. 1998).

## 7. Data pre-processing

All input layers were transformed to a 50 km x 50 km cell size. Layers with a more precise resolution were averaged; conversely, layers with a less precise resolution were interpolated to that size. The model contains 7698 cells of that size. Of these, 71 contain known diamondiferous kimberlites. Each 50 x 50 km cell was assigned "1" if at least one diamondiferous kimberlite is known in that cell, and "0" if not. This forms a binary layer which is used as the target data for neural network training.

Training by a neural network usually requires having subequal numbers of deposits cells vs. "barren" cells. However, the number of available deposits is usually quite low even in the best cases, which means that a difficult choice of barren cells must be made to accommodate the low number of deposits. A technique of noise addition (Brown et al., 2003) can be used to create a number of synthetic, randomly generated deposits for training. This technique has been shown to significantly improve training results.

Here, a noise addition scheme in which 700 hundred synthetic kimberlites have been added using a 20% randomly generated noise has been used. All cells which are not known to contain any kimberlites were considered as "barren".

## 8. Data processing by a feed-forward, back-propagation neural network

A feed-forward, back-propagation neural network of the generalized feed-forward type was trained using the input and target data. The neural networks software used for the training was NeuroSolutions 4.01. As is usual with neural network training, available cells were split into training (50%), cross-validation (25%) and testing (25%) subgroups. The network used had the following characteristics:

- 48 neurons in the input layer
- 8 neurons in the hidden layer
- 8 neurons in the output layer
- Learning algorithm: Quickpropagation with step size 0.04 and a momentum
- 10 runs with 5000 cycles maximum per run, stopping on any increase in the cross-validation mean squared error for at least 50 cycles. The network with the lowest mean squared error in the cross-validation group was kept as the best network and used to produce the maps.

## 9. Results and interpretation

### Classification results on test cells

80% of all barren cells in the test group were classified as barren (Table 1). The remaining 20% are barren cells that are considered favourable by the network. 95% of all diamondiferous kimberlites cells in the test group were correctly classified as favourable. These test results indicate that the neural network is able to compute a combination of input cells that can predict the location of known kimberlites vs. barren areas.

### Sensitivity analysis

Sensitivity analysis is a method that can be used to semi-quantitatively rate the importance of inputs. Results of the sensitivity analysis are presented on Figures 7 and 8. The most favourable areas are characterized by fast velocities and high horizontal gradients in the lower parts of our tomographic model (150 to 230 km depths), high wave velocities in the middle-upper parts (50-90 km) and low Bouguer gravity anomalies.

Table 1

Output / Desired	Deposit	Barren
Deposit	158	381
Barren	27	1531
<b>Performance</b>	<b>Deposit</b>	<b>Barren</b>
Mean Squared Error	0.13	0.13
R	0.45	0.45
Percent Correct	85.4	80.0

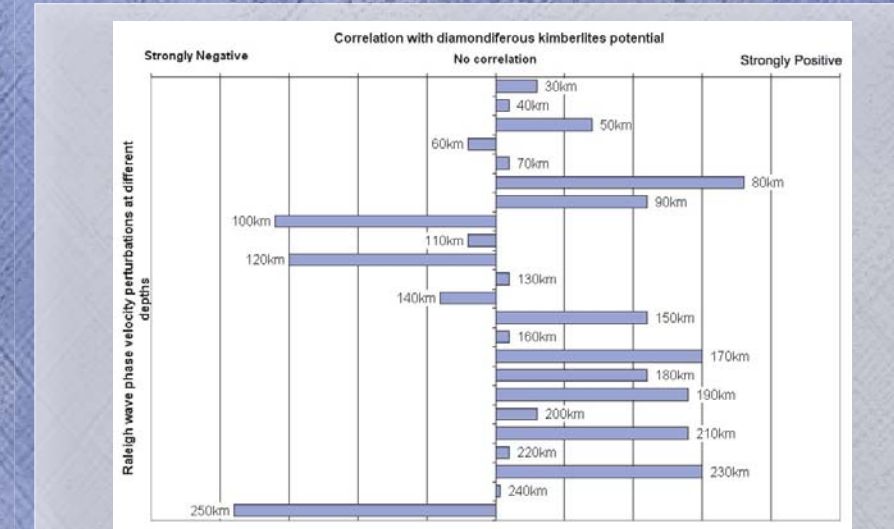


Figure 7: Sensitivity analysis for raw Raleigh wave phase velocity perturbations.

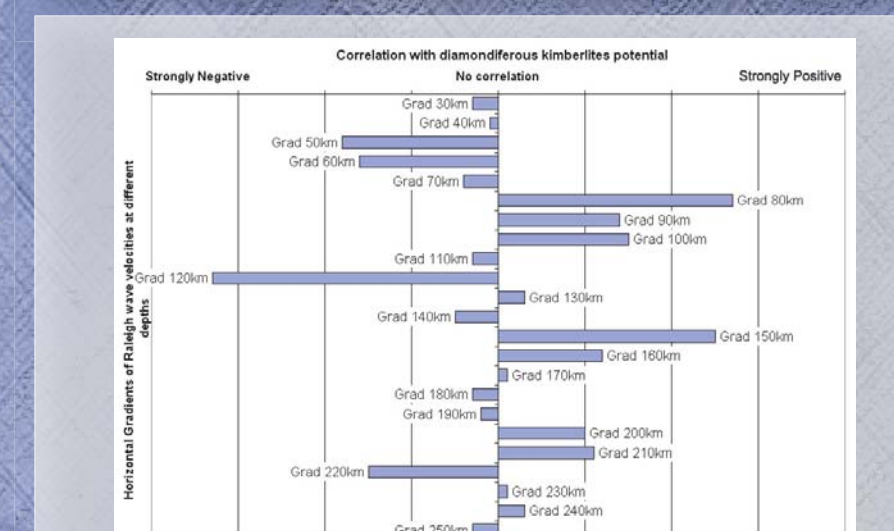


Figure 8: Sensitivity analysis for horizontal gradients of Raleigh wave phase velocity perturbations.

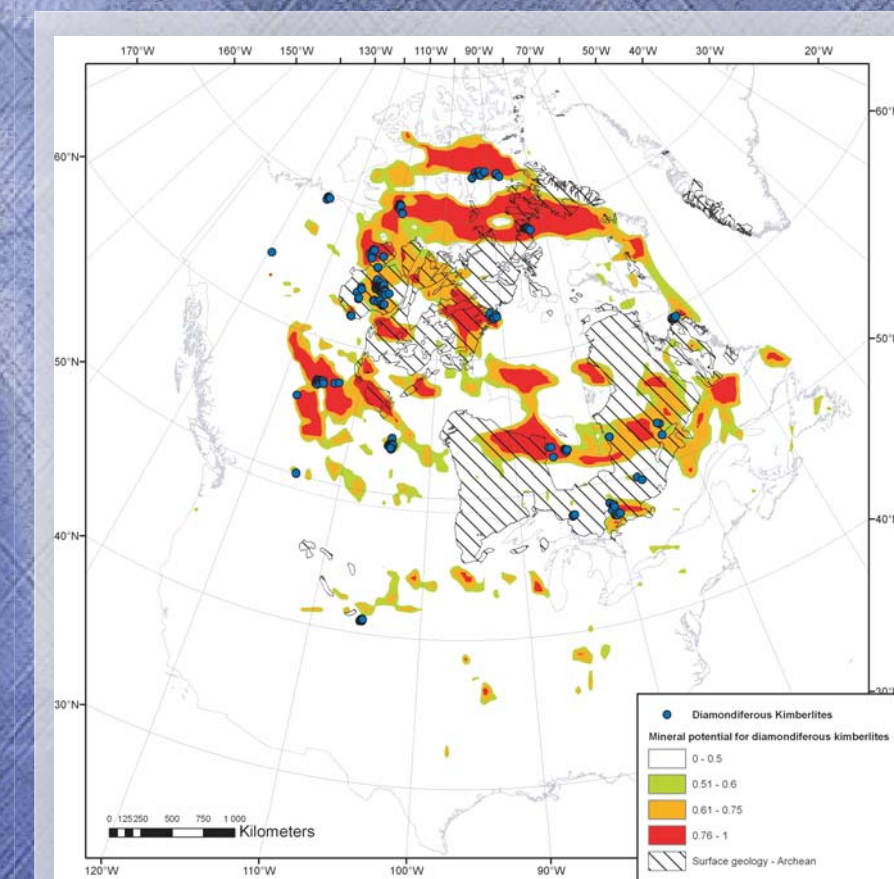


Figure 9: Mineral potential for diamondiferous kimberlites in North America.

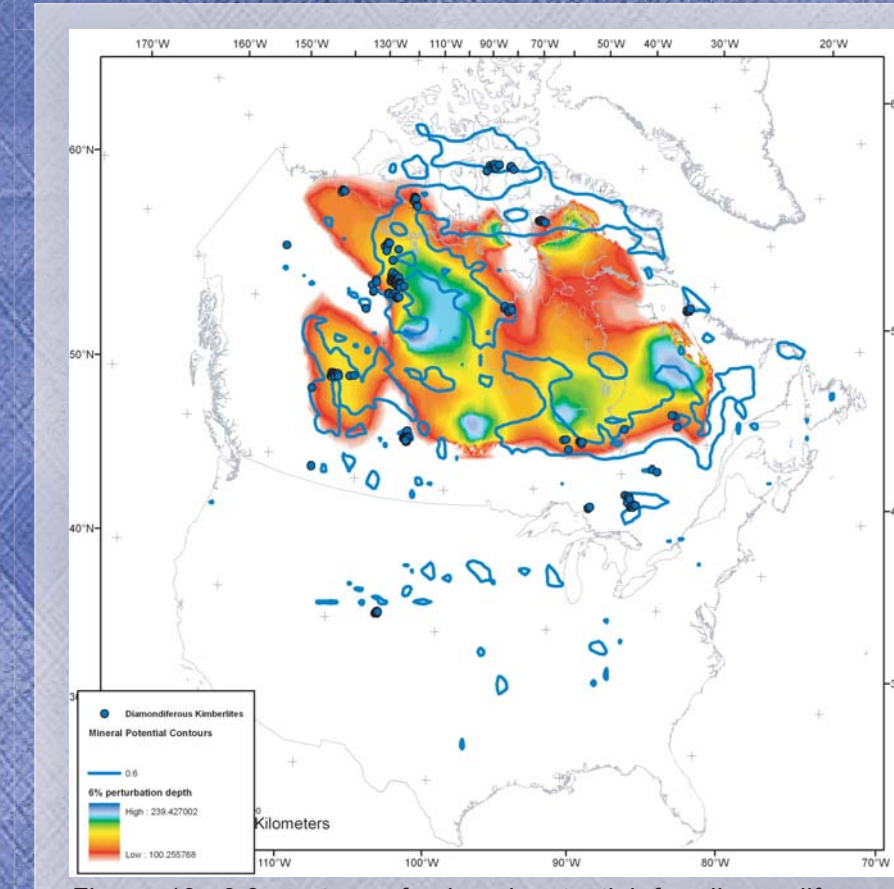


Figure 10: 0.6 contour of mineral potential for diamondiferous kimberlites in North America superimposed on a raster of the depth at which a +6% wave velocity perturbation is attained.

## Discussion and interpretation

The Mineral potential for diamondiferous kimberlites in North America is shown on Figure 9. The high favourable regions for diamondiferous kimberlites are not vertically correlated with coldest and deepest part of the cratons, but surround high velocity roots at depths between 160 to 200 km (Fig. 10). This observation broadly supports the hypothesis that kimberlites are confined to the margin of cratons (Kennedy, 1985; Griffin et al., 2004), but we further suggest that the most favourable areas are located around cratonic keels between that range of depths (Faure et al., 2006). In particular, that is prevalent underneath Slave-Rae-Hearne cratons where Lac de Gras and Rankin Inlet fields are located on west and east sides respectively of a circular region of high favorability.

One particularly interesting feature on the resulting mineral potential map is the presence of a large, E-W trending, high favorability zone that connects the Hudson Bay lowlands kimberlites in Ontario (Attawapiskat) with the James Bay and Otish kimberlites in Quebec (Fig. 9). The Grenville Parautochthonous zone in central Quebec and Labrador also appears as a favourable regional target.

Our correlation results for intervals between 150-230 km are in accordance with the depth of the diamond stability field and the Lithosphere-Asthenosphere boundary (LAB) estimated by xenoliths in kimberlites (Griffin et al., 2004; Fig. 7). The strong association with high horizontal gradients (depths 80 and 150 km) further indicates that the most prospective terrains are those that are at the boundaries between different thermal/compositional blocks or deep seated mantle structures.

## References

Bougrain, L., González, M., Bouchol, V., Cassard, D., Lips, A.L.W., Alexandre, F., Steyn, G., 2003. Knowledge Recovery for Continental-Scale Mineral Exploration by Neural Networks. *Natural Resources Research*, 12, no 3, pp.173-181.

Brown, W., Graves, D.I., Gedeon, T., 2000. Artificial Neural Networks: a new method for mineral prospectivity mapping. *Australian Journal of Earth Science*, no 47, pp.737-749.

Brown, W., Gedeon, T., Graves, D.I., 2003. Use of Noise to Augment Training Data: a Neural Network Method of Mineral-Potential Mapping in Regions of Limited Known Deposits. *Examples, Natural Resources Research*, 12, no 2, pp.141-152.

Clowes, R.M., Hammer, P.T.C., Fernández-Viayo, O., and Welford, J.K., 2005. Lithospheric structures in northwestern Canada from LITHOPROBE seismic refraction and related studies: A synthesis. *Can. J. Earth Sci.* 42, 1277-1293.

DNAG Gravity Anomaly Map of North America. *Geophysics of North America CD-ROM*, National Geophysical Data Center, 1989.

Faure, S., 2006. World Kimberlites and Lamproites CONSOREM Database (Version 2006-1). Consortium de Recherche en Exploration Minière CONSOREM, Université du Québec à Montréal. Numerical Database on www.consorem.ca.

Faure, S., Godsy, S., and Fallora, F., 2006. A new guide for regional correlation of diamondiferous kimberlites using 3D tomography of the North American lithospheric mantle. *GAC-MAC Abstract*.

Godsy, S., Sneider, R., Villaseñor, A. and Benz, H., 2003. Surface wave tomography of North America and the Caribbean using global and regional broad-band networks: phase velocity maps and limitations of ray theory. *Geophysical Journal International*, 152, 620-632.

Griffin, W.L., O'Reilly, S.Y., Doyle, B.J., Pearson, N.J., Cooper-Smith, H., Kivi, K., Malocheva, V., Pokhilenko, N., 2004. Lithosphere mapping beneath the North American plate. *Lithos* 77 (1-4):873-922.

Kennedy, W.O., 1985. The influence of basement structure on the evolution of the coastal (Mesozoic and Tertiary) basins. In: *Int. D.C. ed., Salt basins around Africa*. The Institute of Petroleum, London, p. 7-16.

Mooney, W.D., Laske, and Masters, Crust 5.1: a global crustal model at 5° degrees. *JGR*, 103, 727-747, 1998.

Singer, D.A., Kouda, R., 1996. Application of a feedforward neural network in the search for Kuroko deposits in the Hokuroko district, Japan. *Mathematical Geology*, 28, pp.1017-1023.

## Acknowledgments

We would like to thank the following individuals for their essential contribution on this project: Stéphanie Godsy for the 3D tomographic model, Francine Fallara for the 3D representation of the tomography and Marie-Line Tremblay and Claude Dallaire for the drafting of this poster.

*Un outil  
pour le développement  
de l'industrie minière  
au Québec*